A Wearable and Implantable UWB Antenna for Brain Computer Interface

Ahmet Bilir*, Katjana Ladic†, Kamran Sayrafian‡, Sema Dumanli§
*École Polytechnique Fédérale de Lausanne, Lausanne, Switzerland
†GBS Solutions, Maryland, USA
‡National Institute of Standards & Technology, Maryland, USA
§Bogazici University, Istanbul, Turkiye, sema.dumanli@bogazici.edu.tr

***Abstract*—In this paper, a pair of implant and wearable antennas for brain–computer interface applications are proposed. The implant antenna, designed as a slotted patch, is embedded within the human skull. The receiver antenna is considered to be located on top, outer rim of the left ear and envisioned to act as a relay to capture and retransmit neural data. The antennas operate in lower Ultra-WideBand frequency range, allowing for higher data rates required for dense spatiotemporal sampling of the brain neural activity. The communication performance between the implant and wearable antennas is evaluated for two implant locations (i.e., vertex area of calvaria and temporal region). It is shown that under worst-case scenario and given the regulatory limit on specific absorption rate, the received signal power is around -57.9 dBm. This is above typical UWB receiver sensitivity; therefore, reliable communication with the wearable receiver is feasible.**

***Index Terms*—brain computer interface, implant antenna, wearable antenna, ultra wideband**

I. Introduction

A Brain Computer Interface (BCI) system is a communication system in which brain signals are read and processed by a computing device. The output from the computing device may further be used to control an external device, either virtual or physical [1]. BCI is a multidisciplinary research area that has drawn considerable attention in recent years due to its attractive and transformative applications across many verticals including healthcare. It is expected to have a considerable impact on treatments of neural function impairments. A BCI typically measures neural activity through electrodes that are implanted either inside the brain or over the brain surface (invasive) or placed externally on the scalp (non-invasive). Although invasive BCI involves medical risks and complications, it offers significantly higher temporal and spatial resolution compared to non-invasive BCIs.

Application of wireless interfaces for brain signal acquisition not only enhances the usability of the BCI system but also facilitates the development of platforms that further integrate the brain with other physiological signals. Invasive BCI is considered as use-case within the scope of the Task Group 6ma (TG 6ma) which is currently conducting a revision of the IEEE international standard in Body Area Networks (IEEE 802.15.6) [2]. Specifically, the task group is considering an Ultra-WideBand (UWB) physical layer that can support high data rate transmissions for dense spatiotemporal sampling of the brain neural activity.

The wireless channel between the brain implant and an external receiver is the core communication link in an invasive BCI system. Therefore, maintaining its reliability is crucial and involves design of efficient antennas. Development of such antennas is challenging for several reasons. First, the human body is a harsh medium for electromagnetic wave propagation due to the high conductivity and inhomogeneous nature of biological tissues. Additionally, the implant antenna must be biocompatible and physically very compact to enable practical implantation. This limits the radiation efficiency and communication range of the antenna.

Several studies in literature have tried to address these challenges. In [3], a dual-band monopole implant antenna with an overall size of 15 mm × 20 mm × 1.6 mm and operating in the 2.4 GHz ISM band as well as the 4.1 GHz to 11.5 GHz range is presented. However, the influence of integrated electronics and the communication performance of the antenna with an external receiver have not been considered. A wide-slot antenna operating in the 3.5 GHz to 4.5 GHz frequency range for brain implant has been proposed in [4]. In their design, the authors use glycerin as an insulating medium to reduce near-field losses. While promising antenna performance is expected, the communication performance of this antenna is not analyzed.

In [5], the authors present an implant antenna operating from 3 GHz to 14 GHz with a compact size of 10 mm × 9 mm × 0.7 mm. The total size of the implanted device, including dummy electronics and packaging, is considered to be 23.5 mm × 13 mm × 4.4 mm. In their design, the authors used water encapsulation as a superstrate layer to load and miniaturize the antenna. Using an ideal half wave dipole off-body antenna, a link budget analysis is performed as a function of the dipole-to-implant distance. The study shows that off-body communication could be possible at 20 cm, 1 m, and 2.4 m; however, this assumes that the off-body antenna is located along the broadside direction of the implant antenna.

Using a classical printed, circular arm, monopole implant antenna, authors in [6] investigated off-body communication with a receiver placed near the implant. Their simulation results indicate a pathloss between 36 and 58 dB for the frequency range 6.5 GHz to 7 GHz; however, the authors note

that the result is heavily influenced by the location, relative distance, and orientation of the two antennas. The authors also conducted ex-vivo experiments by inserting the implant antenna in a 15-mm-thick, multilayer skin/fat porcine tissue. They reported a pathloss of 52 dB at the frequency of 6.7 GHz when the receiver is 10 cm away from the implant.

In [7], [8], authors evaluate the communication performance of the BCI channel between the implant and an on-body antenna. In their set-up, the on-body antenna is placed directly above the implant, resulting in a separation distance of approximately 3.5 mm to 10 mm. The frequency range of 3.1 GHz to 10.6 GHz has been considered for link evaluation. At 3 GHz, a transmission coefficient of –10 dB is observed when the antennas separation is 3.5 mm.

Assuming that the brain implant is designed to be placed in the backside of the ear and just below the skin, authors in [9] present an on-body receiver antenna that is formed around a standard earbud (approximately 10 mm away from the implant). The UWB BCI channel is evaluated using computational model of the head and the result show a transmission coefficient of around –35 dB across 3.6 GHz to 6.8 GHz frequency range.

In [10] a dual-band printed monopole antenna with dimensions 22 mm × 24 mm for bidirectional BCI application has been proposed. The authors also evaluate the communication performance of this antenna by placing the receiver antenna directly above the implant (located under the skull) with a distance of 10 mm from the surface of the skin. The distance between the two antennas in their simulation model has been assumed to be 20 mm. In this configuration, the authors report a transmission coefficient of around -35 dB across the 3 GHz to 6 GHz frequency range.

The very limited communication range of the brain implant and especially the heavy dependency of this range on relative position and orientation of the off-body receiver antenna as well as the complex propagation environment could result in limited communication mobility of the individuals that require BCI. To avoid potential restriction in mobility, an on-body relay node can be introduced to capture the signal from the brain implant and retransmit the data to another external node or portable device such as a smart phone. Using this concept, we propose a BCI communication link where the external node is an on-body device located on top of the ear. The device, for example, can be mounted on the arm of an eyeglass (i.e., the temple) or incorporated as part of an earpiece. This will avoid any undesirable wearables on top of the head and allow for convenience and enhanced practicality for frequent or extended use.

The remainder of this paper is organized as follows. Section II describes the implant and on-body antennas that have been designed for BCI applications. Simulation results indicating the communication performance of the antenna and a preliminary link margin analysis are presented in Section III. Finally, conclusions and future work are provided in Section IV.

II. Implant and On-body Antenna Design

The implant device consists of three main parts: electronics, antenna, and encapsulation. Its overall dimensions are assumed to be 15 mm × 15 mm × 6 mm. To minimize the influence of electronics on antenna performance, a patch antenna has been selected. For biocompatibility, the electronics are considered to be enclosed in a titanium casing and placed below the ground plane. Alumina is used as the antenna superstrate. Due to its high permittivity and low loss, alumina enables antenna miniaturization with lower near-field losses. To enhance the antenna bandwidth, U-shaped slots are introduced on the patch. A low-permittivity substrate, RO5880 ($\epsilon_r = 2.2$), with a thickness of 1.57 mm, has also been used. Fig. 1 shows the geometry of the implant antenna.

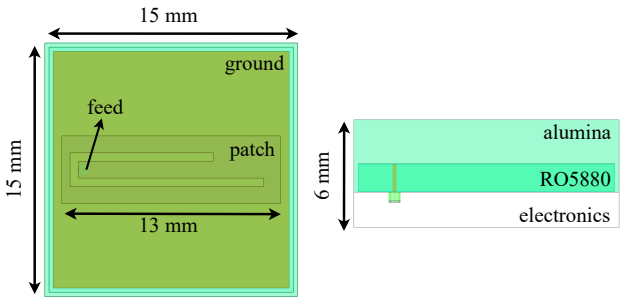

Fig. 1. The geometry of the implant

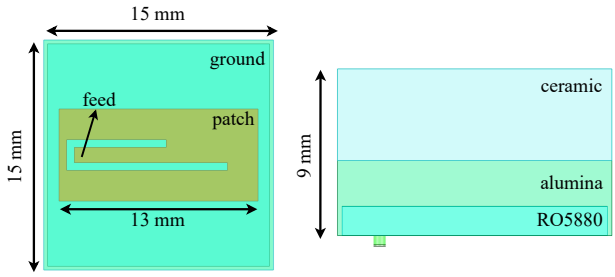

Fig. 2. The geometry of the on-body antenna

The on-body antenna is designed to achieve a directional radiation pattern. Similar to the implant antenna, a U-shaped slotted patch configuration is employed for the on-body antenna. A high-permittivity ceramic substrate ($\epsilon_r = 30$) has also been used to enable miniaturization. The overall dimensions of the on-body antenna are 15 mm × 15 mm × 9 mm. The antenna geometry is shown in Fig. 2.

III. Simulation Results and Analysis

The computational models used to assess antennas performance are shown in Fig. 3. The on-body antenna is positioned on top, outer rim of the left ear (i.e., helix of the left ear). For the implant antenna location, two scenarios have been considered. In the first scenario, the implant is placed within the vertex area of Calvaria (i.e., inside the skull bone). In the second scenario, the implant is moved to the left temporal

region of the skull (i.e., the left side of the head). These two scenarios for the BCI implant positions are also being considered by the task group 6ma at IEEE802.15.

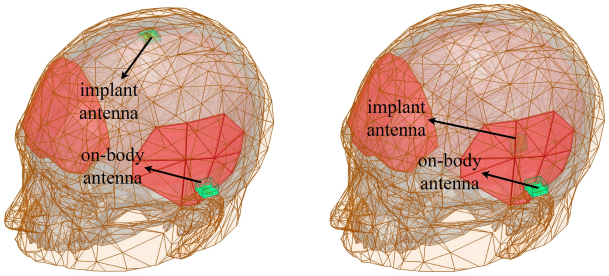

Fig. 3. Computational models used to assess the communication link between the implant and on-body antennas, (a) Implant at the vertex area of Calvaria, (b) Implant at the left temporal region of the head

The S-parameters for scenario 3(a) are presented in Fig. 4. The implant antenna exhibits a –10 dB bandwidth from 3.6 GHz to 5.6 GHz, while the $|S_{22}|$ indicates the operating frequency range of 4.05 GHz to 5.17 GHz for the on-body antenna. In this frequency range, the transmission coefficient $|S_{21}|$ varies between –58 dB and –78 dB; and remains higher than –66 dB below 4.50 GHz. The radiation characteristics of both antennas are also analyzed. Fig. 5 shows the gain patterns of the implant and on body antennas at 4.5 GHz. The peak gain of the implant and on-body antennas are –13.8 dBi and 0.2 dBi, respectively. Similarly, the S-parameters for scenario 3(b) are presented in Fig. 6. As expected, the reflection coefficients of both antennas remain nearly unchanged; however, the transmission coefficient increases. Within the 4.05 GHz to 5.17 GHz frequency range, the transmission coefficient varies between -38 dB and –48 dB.

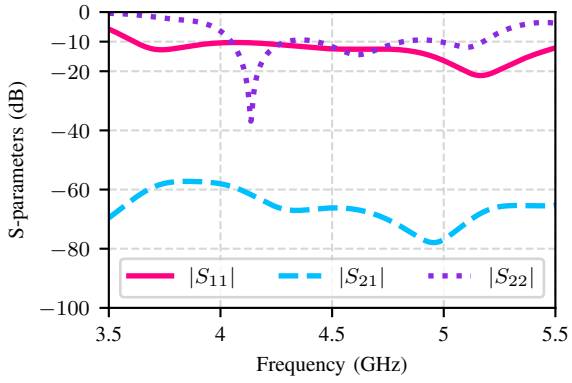

Fig. 4. The S-parameters obtained from the computational model in Fig. 3(a)

To investigate whether the minimum signal strength needed for reliable communication can be achieved in the scenarios shown in Fig. 3, we first need to calculate maximum allowable transmit power. Transmit power is limited by specific absorption rate (SAR) which is a safety limit set by regulatory

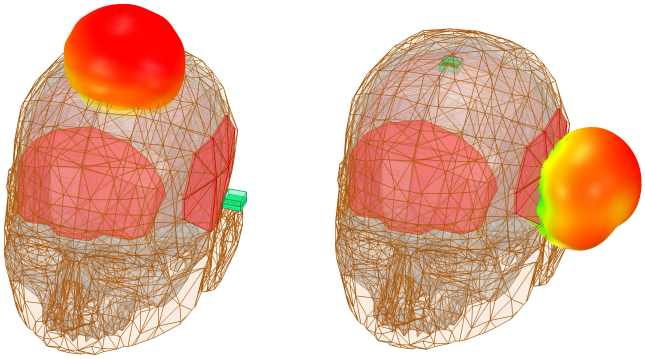

Fig. 5. The 3D gain plot of the implant (left) and the onbody (right) antennas at 4.5 GHz.

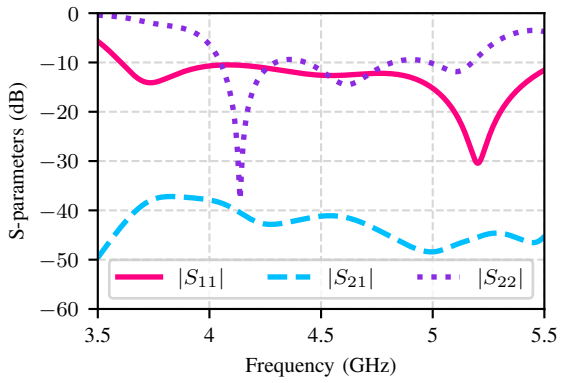

Fig. 6. The S-parameters obtained from the computational model in Fig. 3(b)

organizations. The international limit for SAR (set by ICNIRP) is 2 W/kg averaged over 10 g of tissue [11]; however, Federal Communications Commission (FCC) in the United States has a stricter limit of 1.6 W/kg averaged over 1 g of tissue [12]. We conduct our analysis for both limits while considering transmission frequency of 4.5 GHz. This is approximately the middle of the operating frequency range for both antennas.

When the implant antenna is located at the top of the skull, the maximum SAR averaged over 10 g of tissue (assuming 10 mW of transmit power) is 0.76 W/kg. Given the ICNIRP limit of 2 W/kg, the maximum permissible power will be 26.3 mW, or equivalently 14.2 dBm. The transmission coefficient for this scenario (as observed in Fig. 4) is –66.0 dB. This results in a received signal power of–51.8 dBm at the on-body device. Similarly, for the more restrictive SAR limit of 1.6 W/kg SAR over 1 g, the maximum transmitter power is obtained to be 6.5 mW (8.1 dBm). Again, considering the transmission coefficient of –66.0 dB, a signal power of –57.9 dBm at the on-body receiver can be expected.

When the implant antenna is located at the side of the head, the SAR averaged over 10 g and 1 g of tissue is 0.68 W/kg and 2.30 W/kg, respectively. Accordingly, the maximum permissible transmit power for the implant can be calculated to be 29.4 mW (14.7 dBm) based on the international SAR

TABLE I
SAR AND RECEIVED SIGNAL ANALYSIS AT 4.5 GHZ

	Implant at the top	Implant on the side
SAR over 10 g	0.76 $\frac{W}{kg}$	0.68 $\frac{W}{kg}$
SAR over 1 g	2.46 $\frac{W}{kg}$	2.30 $\frac{W}{kg}$
Max allowed TX Power under 2 W/kg SAR over 10 g	26.3 mW	29.4 mW
Max allowed TX Power under 1.6 W/kg SAR over 1 g	6.5 mW	6.9 mW
Transmission Coefficient at 4.5 GHz	-66.0 dB	-41.1 dB
Received Power under 2 W/kg SAR over 10 g	-51.8 dBm	-26.4 dBm
Received Power under 1.6 W/kg SAR over 1 g	-57.9 dBm	-32.7 dBm

limit and 6.9 mW based on the U.S. SAR limit. Given the transmission coefficient of –41.1 dB at 4.5 GHz (as observed in Fig. 6), this results in the received signal power of -26.4 dBm and -32.7 dBm, respectively. These results are summarized in Table I.

A similar analysis was conducted to investigate the received signal power under worst case channel scenario. The lowest magnitude of the transmission coefficient ($|S_{21}|$) of the BCI channel is -77.9 dB which occurs at the frequency of 4.95 GHz for the implant scenario 3(a). At this frequency, the maximum SAR averaged over 1 g of tissue is 3.27 W/kg. This translates to a maximum permissible transmit power of 4.9 mW (6.9 dBm). This results in the received power of -71.0 dBm which is above typical UWB receiver sensitivity. Therefore, our analysis indicates that reliable UWB communication for BCI is feasible with an on-body receiver that is located above the ear.

IV. CONCLUSIONS AND FUTURE WORK

Ease-of-use for extended or long-term recordings of brain signals has initiated interest in wireless data communication from a brain implant. In this paper, we investigated the communication channel between a brain implant and a wearable relay node that can be mounted on the arm of an eyeglass or incorporated as part of an earpiece. Given the regulatory SAR limits, we have shown that the minimum received power at the relay node is still above typical UWB receiver sensitivity. This indicates the feasibility of having the proposed wearable device. The relay device can retransmit the neural data to another external computing device that resides further away from the individual with the BCI implant. As the wearable node doesn't have the severe power limitation of the implant, enhanced mobility and extended range for wireless communication with another computing device can be expected.

The wireless channel between the brain implant and an external receiver is the core communication link in a BCI system. Therefore, design of efficient antennas and thorough understanding of the RF propagation in this channel are required to enhance the reliability of the system. In-depth RF propagation study and channel characterization are essential to determine the best wireless transmission technologies for the desired BCI applications. The authors plan to further optimize the on-body antenna to increase its 10 dB bandwidth and also investigate other locations such as behind or below the ears as possible placements for the wearable device. Also, fabrication of the proposed antennas and experimental characterization using phantoms that mimic the electrical properties of human tissues will be done in future studies.

ACKNOWLEDGMENT

This project is supported by the National Institute of Standards and Technology in the United States under the grant number 60NANB23D259.

REMARK

Certain commercial instruments or materials are identified in this paper in order to adequately clarify the research. Such identification is not intended to imply recommendation or endorsement by the respective organizations of the authors.

REFERENCES

[1] Sahonero-Alvarez, G., Singh, A. K., Sayrafian, K., Bianchi, L., Roman-Gonzalez, A. (2021). A Functional BCI Model by the P2731 Working Group: Transducer. Brain-Computer Interfaces, 8(3), 92–107. https://doi.org/10.1080/2326263X.2021.1968633

[2] T. Kobayashi , D. Anzai , M. Hernandez, R. Kohno, M. Kim, S. Asano, Y. Aoki , K. Ladic, K. Sayrafian, "TG6ma Channel Model Document for Enhanced Dependability", IEEE 802.15-22-0519-09-006a, Nov. 2024.

[3] M. Salimitorkamani, H. Odabasi and A. Najafi, "A Dual-Band Microstrip Patch Antenna for Brain-Machine Interface Applications," 2021 15th European Conference on Antennas and Propagation (EuCAP), Dusseldorf, Germany, 2021, pp. 1-5.

[4] T. Dissanayake, K. P. Esselle and M. R. Yuce, "Dielectric Loaded Impedance Matching for Wideband Implanted Antennas," in IEEE Transactions on Microwave Theory and Techniques, vol. 57, no. 10, pp. 2480-2487, Oct. 2009.

[5] S. Imran Hussain Shah, A. Basir, H. Yoo and I. -J. Yoon, "A Compact Ultrawideband Antenna System With Stable Broadside Radiation Patterns for Brain–Machine Interface Applications," in IEEE Transactions on Antennas and Propagation, vol. 73, no. 1, pp. 629-634, Jan. 2025.

[6] M. Song, Y. Huang, H. J. Visser, J. Romme and Y. -H. Liu, "An Energy-Efficient and High-Data-Rate IR-UWB Transmitter for Intracortical Neural Sensing Interfaces," in IEEE Journal of Solid-State Circuits, vol. 57, no. 12, pp. 3656-3668, Dec. 2022.

[7] H. Bahrami, S. A. Mirbozorgi, L. A. Rusch and B. Gosselin, "Biological Channel Modeling and Implantable UWB Antenna Design for Neural Recording Systems," in IEEE Transactions on Biomedical Engineering, vol. 62, no. 1, pp. 88-98, Jan. 2015.

[8] H. Bahrami, B. Gosselin and L. A. Rusch, "Realistic modeling of the biological channel for the design of implantable wireless UWB communication systems," 2012 Annual International Conference of the IEEE Engineering in Medicine and Biology Society, San Diego, CA, USA, 2012, pp. 6015-6018.

[9] R. Saha and S. A. Mirbozorgi, "Earbud-Based UWB Data Link for Multichannel Brain Neural Recording and Stimulation Interfaces," 2022 20th IEEE Interregional NEWCAS Conference (NEWCAS), Quebec City, QC, Canada, 2022, pp. 389-392.

[10] S. Yazdanifard and R. A. Sadeghzadeh, "Investigation of dual-band antenna with low-SAR characteristics for bidirectional brain-machine interface applications," Biomedical Signal Processing and Control, vol. 70, p. 102978, Sep. 2021.

[11] International Commission on Non-Ionizing Radiation Protection, "ICNIRP guidelines for limiting exposure to electromagnetic fields (100 kHz to 300 GHz)," Health Phys vol 118(5), pp. 483–524, 2020.

[12] Federal Communications Commission, "Guidelines for Evaluating the Environmental Effects of Radiofrequency Radiation," FCC Report and Order 96-326, Aug. 1996.